© Universiti Tun Hussein Onn Malaysia Publisher's Office

IJIE

Journal homepage: http://penerbit.uthm.edu.my/ojs/index.php/ijie
ISSN : 2229-838X e-ISSN : 2600-7916

The International Journal of Integrated Engineering

Fuzzy Model Reference Adaptive Controller for Position Control of a DC Linear Actuator Motor in a Robotic Vehicle Driver

Ammar A M H Mahdi, W S I W Salim*, Kahlan H M Farhan

Faculty of Mechanical and Manufacturing Engineering,
Universiti Tun Hussein Onn Malaysia, 86400 Batu Pahat, MALAYSIA

*Corresponding Author

DOI: https://doi.org/10.30880/ijie.2020.12.03.027
Received 20 December 2019; Accepted 31 January 2020; Available online 27 February 2020

Abstract: This paper presents the controller development for DC linear actuator motors that are used to control the throttle and brake pedals of a passenger car with automatic transmission. The Fuzzy Model Reference Adaptive Control (Fuzzy MRAC) system allows the vehicle to follow speed vs. time profiles of driving cycles by dynamically adjusting the position of the driver pedals in a vehicle. The designed controller was implemented to a virtual vehicle model to determine the required position of the linear pedal actuators over a standard driving cycle. The driving-cycle simulation was conducted using Matlab Simulink and the performance of the controller was analyzed based on overshoot, rise time, settling time and mean square error whereas the robustness test was carried out via set-point tracking method. The result shows 19.79 s rise time, 0.1619% overshoot, 32.65 s settling time and 0.0041 mean square error. The results have proven Fuzzy MRAC to be a viable option for use in highly dynamic systems suchas automotive standard driving cycle controllers.

Keywords: Robotic driver, DC linear actuator motor, Fuzzy Model Reference Adaptive Controller, driving cycle, Matlab Simulink, vehicle model.

1. Introduction

There have been expeditious developments in mechatronics, factory automation, and robotic systems where the necessity for intelligent controllers become high [1]. The good position accuracy, higher linear force densities and a smooth motions are the essential requirements in most robotic applications [2]. DC motors actuator are widely used in the industry, especially in robotic applications. A specific example of this application is the use of a robotic driver to control the position of vehicle pedals in standard vehicle driving cycle tests [2][3][4][5]. The actuators using DC linear motors in this type of application are subjected to many disturbances caused by uncertain working environments. Several control approaches have been considered by researchers for developing robotic driver [4]-[12]. Existing controllers are largely based on traditional PID types which vary from one application to another in terms of accuracy and range of operation [4]-[12]. In reference [5], a robotic driver was designed and developed using single linear motion to actuate the brake and throttle pedals controlled by two cascaded PID controllers (vehicle speed and pedal actuator position). The authors suggested the use of Fuzzy PID to overcome the system limitations such as motor saturation and accelerator pedal stick-slip. Very few literature reports on the use of artificial intelligence (AI) controller system in robotic driver's application [8]. A simple conventional controller is not sufficient to deliver the required precision needed in driving cycle tests. Therefore, a control method that adapts the DC linear actuator motor to various driving patterns while maintaining system performance without parameter resets is needed. For this purpose, the Fuzzy Model Reference Adaptive Controller (Fuzzy MRAC) is proposed to overcome the stability and accuracy of the positioning of the linear actuator. In this article, the modeling method which involves the derivation of the mathematical equations for the

*Corresponding author: wsaiful@uthm.edu.my

electromechanical system and the transfer function for the DC linear actuator motor is discussed. The DC motor used in this study comprises a planetary gearhead and a loaded lead-screw, which transform the angular displacement of the motor to linear movement to press and depress (or release) the vehicle pedals based on a standard driving cycle. The DC linear actuator controller model is implemented in a virtual vehicle model to identify the positions of the vehicle pedals based on the New European Driving Cycle (NEDC) pattern on the chassis dynamometer [13].

2. Methodology

The current work involves the design of Fuzzy MARC employed in a vehicle robot driver (DC linear actuator motor). This section describes the overall system starting from the system description and the Fuzzy MRAC designed based on the obtained transfer function that represent the physical characteristics of the DC linear actuator through mathematical modelling.

2.1 System Description

The design of the robot driver has been developed based on the selected DC linear actuator motor as shown in Fig.1. The robot driver will be placed on the floor of the vehicle in the front legroom space behind the vehicle's pedals. The linear motion of the actuator motor is required to press and depress the vehicle pedals based on the selected standard or regional driving cycle.

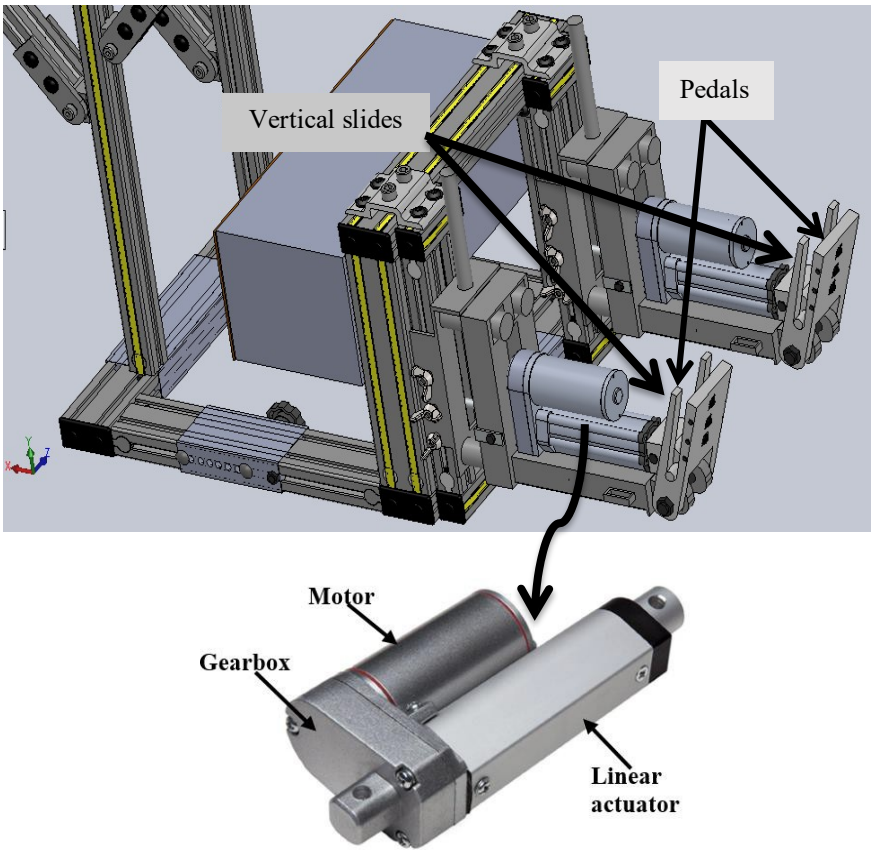

Fig. 1 - Schematic diagram of vehicle robotic driver and the DC linear actuator motor mechanism

The DC motor (Model HB-DJ806) is used for position or speed control in closed loop control systems. The mathematical modelling for the DC motor is required to obtain the transfer function that represents the characteristics of the system. The transfer function of the DC motor should be determined first before designing the controller using Matlab Simulink. The electric equivalent circuit of the armature and the free-body diagram of the rotor are shown in Fig.2 (a). The armature is modelled as a circuit with resistance, (Ra) connected in series within inductance, (La) and a voltage source, (Vb(t)) represents the back electromagnetic force (EMF) in the armature when the rotor rotates [14][15][16].

The transfer function for the DC motor is derived using differential equations based on Newton's second law as shown in Equation (1), where the typical equivalent mechanical loading on a motor that is connected to the motor shaft includes total moment of inertia, J_m and total viscous friction B_m. T(t) is the torque developed by the motor. The Kirchhoff's voltage law shown in Equation (2) represents the state of the dynamics of the DC motor system.

$$(t) = J_m s^2 \theta_m + Bs(t) \quad (1)$$

$$(t) = I(t)R_a + V_b(t) \quad (2)$$

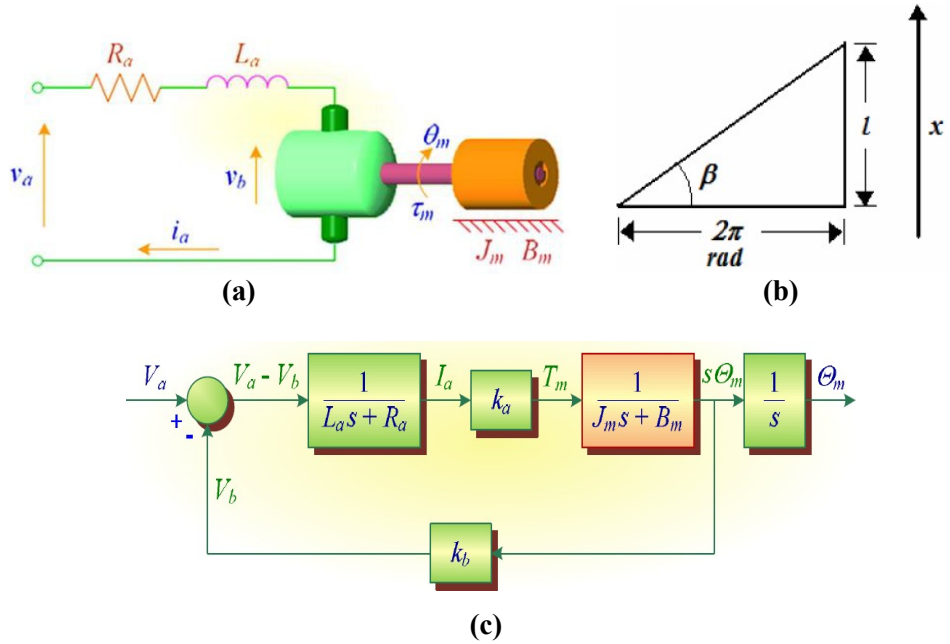

Fig. 2 - DC motor system: (a) Schematic diagram of motor circuit (b) Relation between angular and linear movement (c) Block diagram of controller system [15]

Equations in (1) and (2) are changed to the frequency domain using the Laplace transform in order to obtain the transfer function as shown in Equation (3) and the block diagram of the control system in Fig.2 (c). The transfer function obtained for the DC motor is for controlling rotational angle. On the other hand, the vehicle robotic driver is required to operate via linear movements. Due to that, the conversion angular to linear displacement is required. Fig.2 (b) shows the relationship between the angular advance caused by the motor and the linear advance after the lead-screw. In this case, **β** represents the angle of the lead-screw lead, **l** represents the step of the lead and **x(t)** is the linear advance. The relationship of angular to linear displacement shown in Equation (4) where $\boldsymbol{P = 2\pi/l}$.

$$\frac{\theta(s)}{E_a(s)} = \frac{k_T}{L_a J_m S^2 + (R_a J_m + B_m L_a)S + (k_T k_E + R_a B_m)} \quad (3)$$

$$\frac{X(s)}{(s)} = \frac{k_T}{P(L_a J_m S^2 + (R_a J_m + B_m L_a)S + (k_T k_E + R_a B_m))} \quad (4)$$

Table 1 - DC linear actuator motor parameters

Parameter	Nomenclature	Value
J_m	Motor armature moment of inertia	1.8375 kg ㎡
k_T	Constant of torque of motor	0.048 Nm/A
k_E	Back EMF constant	0.048 Vs/rad
R_a	Armature resistance	4.385Ω
T	Motor torque	0.062 Nm
I_a	Armature current	1.3A
B_m	Viscous friction coefficient	0.4-0.5 Nms/rad
L_a	Electric inductance	2 H

The parameters associated with the DC linear actuator motor used in this simulation is shown in Table 1. These values are substituted in Equation (4) to obtain the system dynamic transfer function given by Equation (5). The distance

for linear displacement is 50 mm based on selected motor specification and the denominator of Equation (5) is multiplied with $\frac{1}{1.26\,s}$ to convert the rotational displacement to linear displacement.

$$\frac{\theta(s)}{E_a(s)} = \frac{0.048}{3.675\,S^2+9.06\,S+\,2.194804} \tag{5}$$

2.2 Fuzzy Model Reference Adaptive Control

Fuzzy model reference adaptive controller is designed based on the plant transfer function obtained in Equation (5). The model reference transfer function is calculated using the plant transfer function of the model. The fuzzy controller is designed with 9 rules and three membership function. The block diagram of the Fuzzy MRAC is shown in Fig.3.

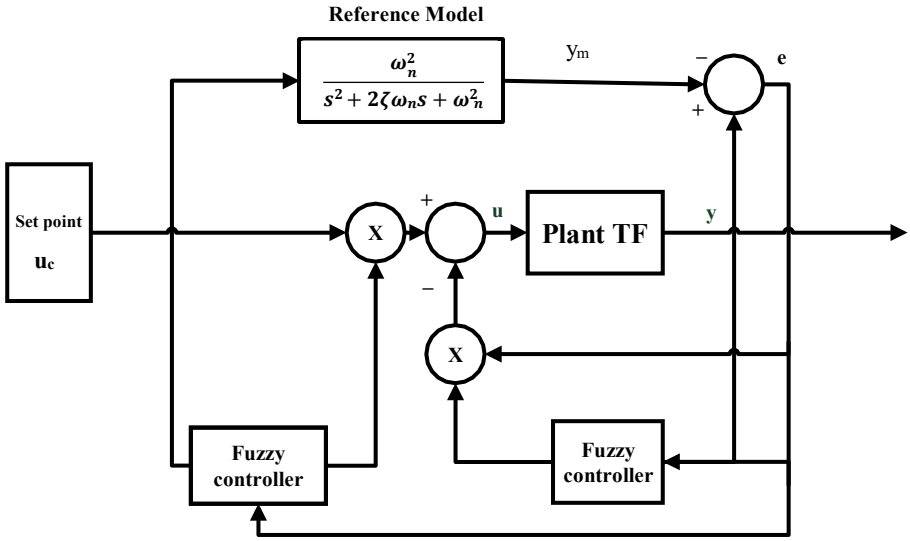

Fig. 3 - System block diagram of Fuzzy MRAC

2.2.1 Model Reference Adaptive Control Transfer Function

The first step taken to obtain the model reference transfer function is by using the settling time of the plant transfer function in Equations (5) and assuming the damping ratio [15]. In order to obtain the settling time of the transfer function, an open loop system test in Matlab software is used. A step input with 50 mm final step value is applied and the system response is obtained in terms of settling time. The settling time obtained from the open loop test is Ts= 24.9189 s. The damping ratio (ζ) is assumed to be 0.95 to represent critical damping [17].

To find natural frequency (ω_n), the equation $\boldsymbol{T_s = \frac{4}{\zeta\omega_n}}$ is used. Thus, ω_n = 0.1689691887. As for reference model, steady state equation is used to obtain the transfer function.

$$G(s) = \frac{\frac{2}{n}}{s^2+2\zeta\omega_n s+\omega_n^2} \tag{6}$$

Substituting the values of ω_n and ζ in equation (6) yields:

$$G_m(s) = \frac{0.029}{s^2+0.3210404585\,s+0.029} \tag{7}$$

Equation (7) introduces the reference model transfer function of the DC linear actuator motor.

2.2.2 Fuzzy Logic controller design

To complete a controller, a few parts in the fuzzy logic are evaluated. Fig.4 shows the block diagram of fuzzy logic controller, which comprises four main parts which include fuzzification, selection of membership function, interface rules development and defuzzification[18].

The information of crisp input from the system will enter fuzzification stage. This stage will convert fuzzy values into fuzzy sets by linguistic expressions. In this work, error and change of error is used [19][20][21][22]. The inputs are then evaluated in terms of the input class with respect to the degree of fulfilment for each class [21]. The inference stage

will decide the rule in terms of linguistic variables to obtain the output of the controller. The rules are developed in the inference stage based on the position of DC linear actuator motor from the input to the output [21]. Finally, the output linguistic variables of membership functions is combined with the controller output magnitude and computed using defuzzification method [21]. From the fuzzy structure, there are two inputs and one output for this system. The two inputs are the error (E) and change of error (CE) and the output is the fuzzification output, which is the fuzzy controller output. The rules and membership functions were designed to ensure that the controllers are suitable. The triangular membership shape is used in this study and the IF-THEN rules are used during the calculation of algorithms [23]. To obtain the design output, the Fuzzy controller is tuned using gain tuning due to its simplicity [18]. Fuzzy 3MRAC describes thecontroller using 3 membership functions with 9 rules. Table 2 shows the rules for Fuzzy 3MRAC. From the rules, NE means negative error, ZE means zero error and PE means positive error. E is for error and CE is for the change of error. This rule is designed to get the optimum performance out of the controller's response.

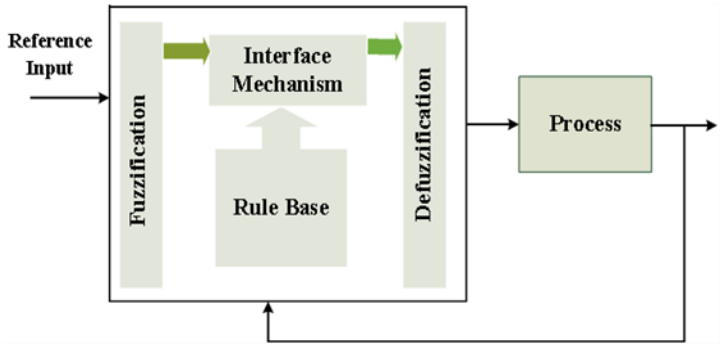

Fig. 4 - Block diagram of fuzzy logic controller

Table 2 -Fuzzy 3MRAC rules for three membership function

		Chang of Error (CE)		
		NE	**ZE**	**PE**
Error (E)	**NE**	NE	ZE	ZE
	ZE	PE	ZE	NE
	PE	ZE	PE	PE

For the input variable error (E) membership function, the range is set from -20.7 to 20.7 and for the input change of error (CE) membership function, the distance is set from 0.4 to 1. Lastly, the distance is set from -1 to 2 for the output membership function. All the membership function consists of triangular shape as shown in Fig. 5 (a), (b), (c) and the surface view of the fuzzy rules in Fig. 5 (d).

In the defuzzification stage, the input is a fuzzy set and the output is a single number. The method used for defuzzification in this study is Center of Gravity (COG). This COG method is the most popular because it returns the centered area under the curve [21]. This method also has fast computation time and is relatively more accurate. Equation (8) represents the COG method, where, U_i is a centre of the output membership function and $\mu(y)$ is the degree of fulfillment.

The performance of the controller is evaluated based on rise time, settling time and the overshoot based on the 2% band [24]. In order to find the performance error for all controllers, the mean square error and root mean square error are considered and calculated based on Equation (9) where y is the actual value and ŷ is the predicted value.

$$U = \frac{\sum_{i}^{1}=1\ U_i\,(y)}{\sum^{i}=1\ (y)} \tag{8}$$

$$M = \frac{1}{t} \sum_{i=1}^{t} (y - \hat{y})^2 \tag{9a}$$

$$RMSE = \sqrt{\frac{\sum_{i=1}^{t} (y-\hat{y})\text{^}2}{t}} \tag{9b}$$

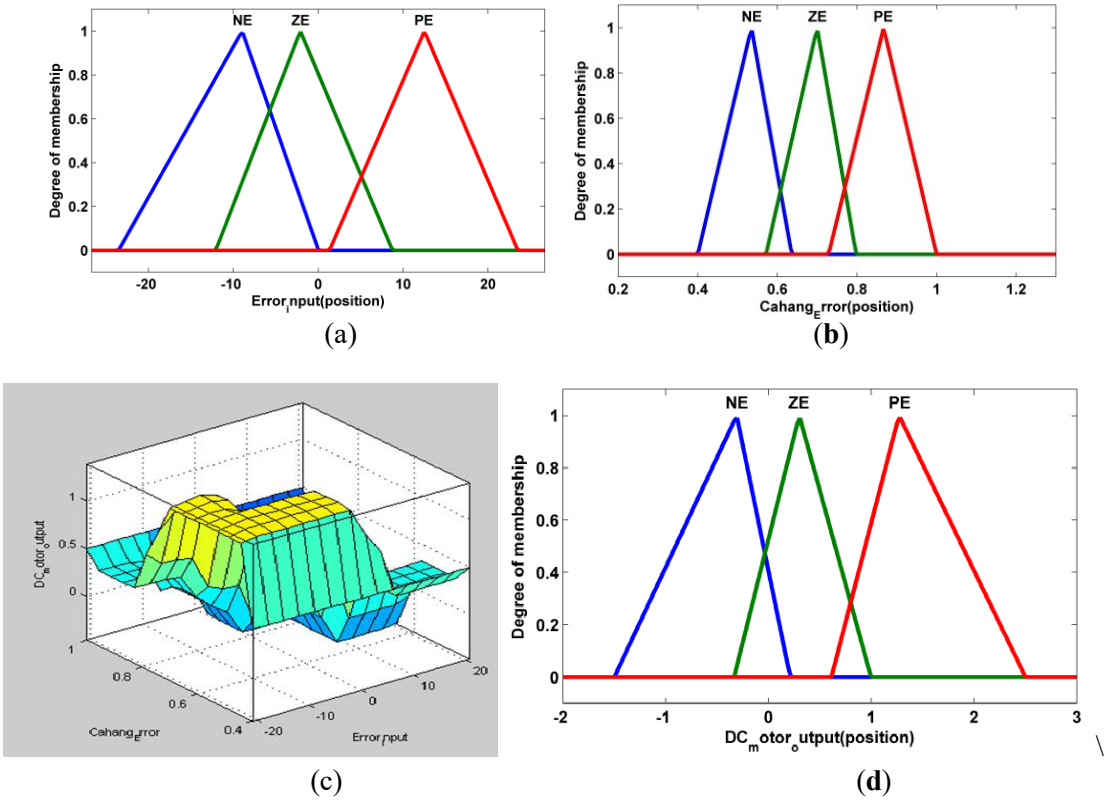

Fig. 5 - Fuzzy with three Membership function: (a) input Error membership function, (b) input Change of Error membership function, (c) output membership function (d) Surface view of fuzzy design

3 Results and Discussion

The analysis of the control system implementation for the DC linear actuator based on the step input and the step input tracking is described. In addition, a combination of the vehicle model and DC linear actuator model is discussed in the following sections.

3.1 Performance of Motor Controller

The design of the DC linear actuator motor to control movements of the pedals is implemented. The fuzzy control is tuned several times in order to get the best performance of the vehicle's throttle and brake position controller response. To do this, the controller is instructed to follow a step change. The system input is a step input with maximum value of 50 mm based on the chosen DC linear actuator stroke. Fig. 6a shows the step response for the fuzzy 3MRAC of controlling DC linear actuator motor position. The transient analysis of the output response is presented in Table 3. The output obtained 19.79 s rise time, 0.1619% overshoot, 32.65 s settling time which indicates a good controller performance.

Table 3 - Performance evaluation for DC linear actuator motor position controller

Parameter	Value
Rise time(s)	19.79
Overshoot (%)	0.1619
Settling time (s)	32.65
Peak value (mm)	50.08
MSE	0.0041
RMSE	0.064

The error analysis has been done in order to evaluate the quality of the controller. The MSE and RMSE have been estimated for the controller from 20 s to 800 s duration. Fig.6b shows the error performance between actual and reference for Fuzzy 3MRAC. Table 3 shows the value of MSE and RMSE analysis for Fuzzy 3MRAC which was designed to control the DC linear actuator motor position. The calculated values are MSE = 0.0041 and RMSE = 0.064, indicating good performance of the designed controller.

The robustness of the controller performance is evaluated by set point tracking, to test the stability of the controller response. This tracking test is done by dividing the set point into two stages; the first stage is 0-30 mm for the time interval of 0-400 s and the second stage is 30-50 mm for the time interval of 400-800s. The step response of set point tracking for Fuzzy 3MRAC of DC linear actuator motor position for controlling the vehicle's throttle and brake pedals is shown in Fig.7, while the transient analysis of the response is shown in Table 4.

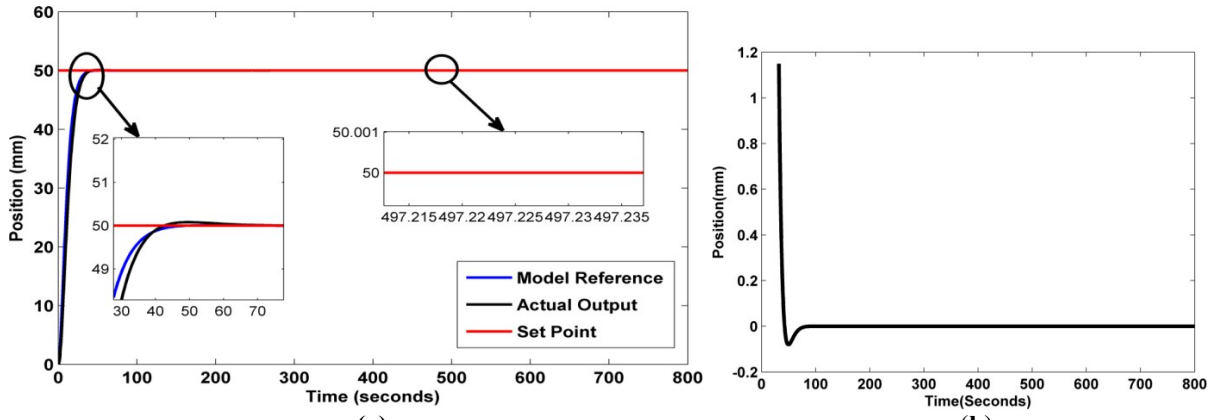

(a) (b)

Fig. 6 - Step response for the DC linear actuator motor position controller (Fuzzy 3MRAC) (b) Error performance between actual and reference position (Fuzzy 3MRAC)

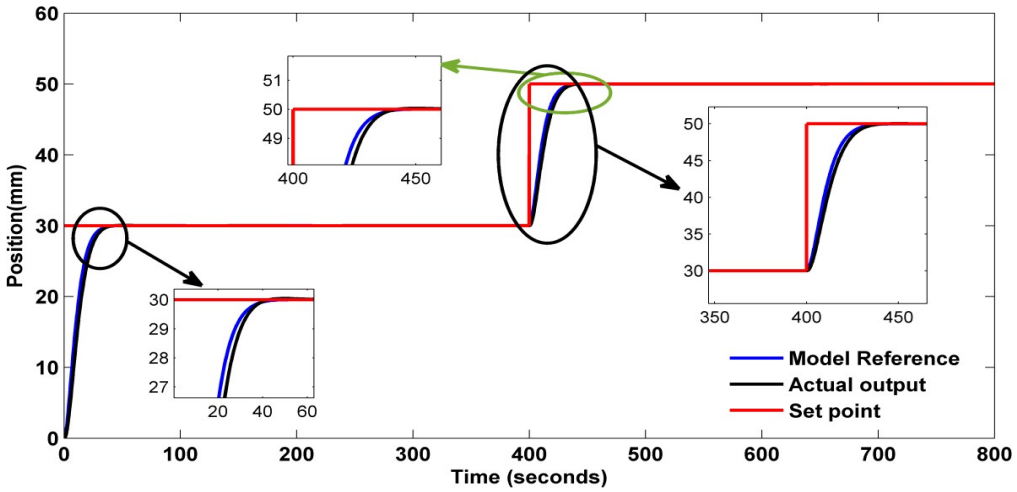

Fig. 7 - Set point tracking response for the position of DC linear actuator motor controller (Fuzzy 3MRAC)

The analysis results in Table 4 shows that the both stages have a similar time response with 19.79s rise time, while the first stage has 0.1619 % overshoot, which is bigger than the recorded overshoot of the second stage (0.0648%). The settling time for the first and second stages are 32.65 s, 432.65 s respectively.

For the error performance value which is a mean square error (MSE) and root mean square error (RMSE). The MSE and RMSE of point tracking are calculated for both stages (32 - 400 s) and (432 - 800 s). Table 4 shows the Fuzzy 3MRAC MSE and RMSE analysis for set point tracking recording 0.0025, 0.0011 MSE and 0.05, 0.033 in the first and second stages respectively.

The overall performance evaluation of the Fuzzy 3MRAC for controlling the position of the DC linear actuator motor indicates that the system is sufficiently stable to be implemented to the actual robotic driver. It is expected that the robotic driver control system will be able to track any imported signal input to the system with high accuracy.

Table 4 - Performance evaluation of set point tracking for DC linear actuator motor position controller (Fuzzy 3MRAC)

First stage (33 mm, 0 < t < 400 s)					
Rise Time (s)	**Overshoot (%)**	**Settling Time (s)**	**Peak value (mm)**	**MSE**	**RMSE**
19.79	0.1619	32.65	30.04	0.0025	0.05
Second stage (50 mm, 400 < t < 800 s)					
Rise Time (s)	**Overshoot (%)**	**Settling Time (s)**	**Peak value (mm)**	**MSE**	**RMSE**
19.79	0.0648	432.65	50.03	0.0011	0.033

3.2 Integrated vehicle and DC linear actuator motor model

A simulated system for the vehicle model and robotic driver model has been run in Matlab Simulink work space. The system is divided into four controllers; two of them controlling the vehicle throttle pedal positions and the other two for brake pedal positions control with both systems working non-simultaneously.

The driving cycle data serves as the input to the system. This feeds into the DC linear actuator motor model which controls the DC linear motor for the brake pedal. The DC motor is connected to the brake module of the vehicle as shown in Fig.8a. The position of the vehicle brake pedal and the vehicle speed is obtained from the simulation and their values are sent back to the DC motor system through a feedback connection. The DC motor then will adjust the pedal accordingly so that the vehicle speed adheres to the input speed from the driving-cycle. Fig.9a shows the position output of pedal displacement /position over the driving cycle. Over the 800 s driving-cycle the recorded maximum displacement of the actuator is 25 mm, which occur four times over the driving cycle. The actual value is expected to differ slightly in actual testing on a dynamometer due to the use of the encoder as position feedback to the Simulink. The position command from encoder will be transferred from Simulink via Arduino Mega Pulse Width Modulation (PWM) which controls the voltage applied to the DC linear actuator motor.

The throttle pedal control model simulation is arranged in a similar manner to the brake model described above. The model is shown in Fig.8b. The output of the throttle pedal displacement output is shown in Fig.9b. It is seen that the output recorded a maximum displacement of 18 mm for the throttle pedal position in the 800 s driving cycle. Again, this may change slightly in actual dynamometer testing for the same reason as that described for the brake pedal system

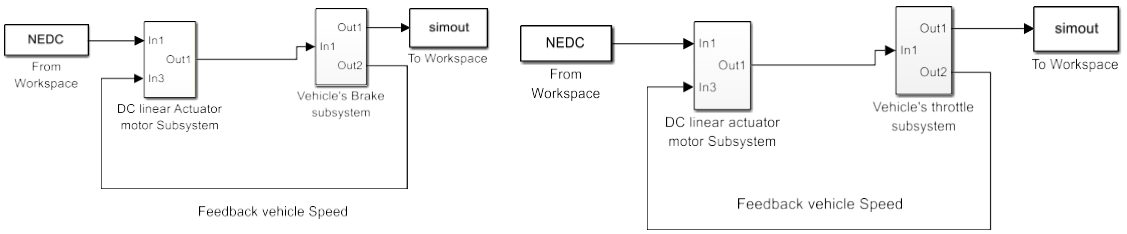

(a) **(b)**

Fig. 8 - Simulated system for the vehicle model and robotic driver model: (a) Simulink system of brake pedal position controller (b) Simulink system of throttle pedal position controller

4 Conclusion

The aim of this study is to investigate the performance of Fuzzy MRAC in providing precise and accurate position control of DC linear actuator motor for vehicle robot driver application. The performance of Fuzzy MRAC evaluation for controlling the DC linear actuator system has been tested on the HB-DJ806 DC motor. The simulation results from step input response indicate that Fuzzy MRAC provide precise and accurate position of DC linear actuator motor. In addition, the robustness performance of Fuzzy 3MRAC to control both linear actuators for brake and throttle pedals has been designed for two different stages and the designed controller shown a good agreement and accuracy to follow various inputs to the system. Furthermore, the vehicle model that has been simulated in Matlab is implemented to the robot driver model (DC Motor system) to ensure of the capability of the designed controller to accommodate the target automotive application. The simulated results demonstrate the capability and stability of Fuzzy MRAC in controlling the vehicle pedals positions for an automatic transmission vehicle following prescribed speeds vs time pattern. In conjunction with the findings, for the future work, the designed controller system will be implemented in an actual robot to drive road vehicles based on selected driving cycles on a chassis dynamometer.

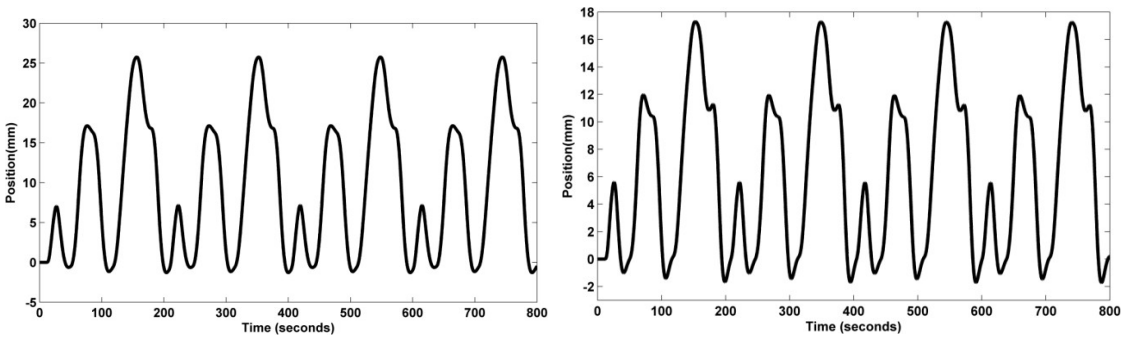

(a) **(b)**

Fig. 9 - (a) Position output of the brake pedal controller (b) Position output of the throttle pedal controller

Acknowledgement

This article was published under the funding by Ministry of Education Malaysia (KPM) through the Fundamental Research Grant Scheme (FRGS 1589), whom the authors wish to acknowledge and thank.

References

[1] Ustun, O., & Tuncay, R. N. (2001). Design, analysis and control of a novel linear actuator. IEMDC 2001 - IEEE International Electric Machines and Drives Conference, 27-32.

[2] Wong, N., Chambers, C., Stol, K., & Halkyard, R. (2008). Autonomous vehicle following using a robotic driver. 15th International Conference on Mechatronics and Machine Vision in Practice, M2VIP'08, 115-120.

[3] Wong, N., Chambers, C., Stol, K., & Halkyard, R. (2009). Development of a robotic driver for autonomous vehicle following. International Journal of Intelligent Systems Technologies and Applications, 8(1/2/3/4),276.

[4] Mizutani, N., Matsui, H., Yano, K., & Takahashi, T. (2018). Vehicle speed control by a robotic driver considering vehicle dynamics for continuously variable transmissions. Journal of Robotics and Mechatronics, 30(2), 300-310.

[5] Namik, H., & Inamura, T. (2006). Development of a robotic driver for vehicle dynamometer testing, In Proceedings of 2006 Australasian Conference on Robotics, 1-9.

[6] Zhu, Z. P., Du, A. M., Ma, Z. X., Zhang, W. Y., & Fan, C. G. (2014). Vehicle Robot Driver Research and Development Based on Servo Motor Control. Applied Mechanics and Materials, 709, 272-275.

[7] Chen, G., Zhang, W. G., & Zhang, X. N. (2013). Speed tracking control of a vehicle robot driver system using multiple sliding surface control schemes. International Journal of Advanced Robotic Systems, 10(2), 90.

[8] Chen, G., & Zhang, W. (2016). Hierarchical Coordinated Control Method for Unmanned Robot Applied to Automotive Test. IEEE Transactions on Industrial Electronics, 63(2), 1039-1051.

[9] Chen, G., & Zhang, W. (2015). Control Method for Electromagnetic Unmanned Robot Applied to Automotive Test Based on Improved Smith Predictor Compensator. International Journal of Advanced Robotic Systems, 12(7), 104.

[10] Sailer, S., Buchholz, M., & Dietmayer, K. (2013). Driveaway and braking control of vehicles with manual transmission using a robotic driver. Proceedings of the IEEE International Conference on Control Applications, 235-240.

[11] Thiel, W., Gröf, S., Hohenberg, G., & Lenzen, B. (2010). Investigations on Robot Drivers for Vehicle Exhaust Emission Measurements in Comparison to the Driving Strategies of Human Drivers. SAE Technical Paper Series, 1, 1922-1929.

[12] Wong, N., Chambers, C., Stol, K., & Halkyard, R. (2009a). Development of a robotic driver for autonomous vehicle following. International Journal of Intelligent Systems Technologies and Applications, 8(1/2/3/4),276.

[13] Salim, W. S. I. W., Mahdi, A. A. M., Ismail, M. I., Abas, M. A., Martinez-Botas, R. F., & Rajoo, S. (2017). Benefits of spark-ignition engine fuel-saving technolog. Journal of Mechanical Engineering and Sciences, 11(4), 3027-3037.

[14] Munadi, & Akbar, M. A. (2015). Simulation of fuzzy logic control for DC servo motor using Arduino based on MATLAB/Simulink. Proceedings of 2014 International Conference on Intelligent Autonomous Agents, Networks and Systems, INAGENTSYS 2014, 42-46.

[15] Munadi, Akbar, M. A., Naniwa, T., & Taniai, Y. (2017). Model Reference Adaptive Control for DC motor based on Simulink. Proceedings - 2016 6th International Annual Engineering Seminar, InAES 2016, 101-106.

[16] Nikhil Shewale, S., & Deivanathan, R. (2018). Modelling and analysis of dc motor actuator for an electric gripper. Journal of Engineering Science and Technology, 13(4), 862-874.
[17] Sharaf, Soliman, Mansour, Kandil, & El-Shafii. (2002, December). Laboratory implementation of artificial neural network speed controller for a rectifier fed separately excited DC motor. 85-88 vol.1.
[18] Ross, T. J. (2010). Fuzzy Logic with Engineering Applications: Third Edition. In Fuzzy Logic with Engineering Applications: Third Edition.
[19] Krejčí, J. (2018). Fuzzy set theory. In Studies in Fuzziness and Soft Computing (Vol. 366, pp. 57-84).
[20] Stankovic, M., Naumovic, M., Manojlovic, S., & Mitrovic, S. (2014). Fuzzy model reference adaptive control of velocity servo system. Facta Universitatis - Series: Electronics and Energetics, 27(4), 601-611.
[21] Iancu, I. (2012). A Mamdani Type Fuzzy Logic Controller. In Fuzzy Logic - Controls, Concepts, Theories and Applications.
[22] Ibrahim, B. S. K. K., Tokhi, M. O., Huq, M. S., & Gharooni, S. C. (2011). Optimized Fuzzy Control For Natural Trajectory Based Fes- Swinging Motion. International Journal of Integrated Engineering, 3(1), 17-23.
[23] Nagarajan, D., Kavikumar, J., Lathamaheswari, M., & Broumi, S. (2019). Intelligent system stability using Type-2 fuzzy controller. International Journal of Integrated Engineering, 11(1), 270-282.
[24] Paraskevopoulos, P. N. (2017). Modern control engineering. CRC Press.